Direct displacement-based design accuracy prediction for single-column RC bridge bents

Giovanni Tecchio[a], Marco Donà[*] and Claudio Modena[b]

*Department of Civil, Architectural and Environmental Engineering (DICEA), University of Padua,
via Marzolo 9, 35131 Padua, Italy*

Abstract. In the last decade, displacement-based (DB) methods have become established design procedures for reinforced concrete (RC) structures. They use strain and displacement measures as seismic performance control parameters. As for other simplified seismic design methods, it is of great interest to prove if they are usually conservative in respect to more refined, nonlinear, time history analyses, and can estimate design parameters with acceptable accuracy. In this paper, the current Direct Displacement-Based Design (DDBD) procedure is evaluated for designing simple single degree of freedom (SDOF) systems with specific reference to simply supported RC bridge piers. Using different formulations proposed in literature for the equivalent viscous damping and spectrum reduction factor, a parametric study is carried out on a comprehensive set of SDOF systems, and an average error chart of the method is derived allowing prediction of the expected error for an ample range of design cases. Following the chart, it can be observed that, for the design of actual RC bridge piers, underestimation errors of the DDBD method are very low, while the overestimation range of the simplified displacement-based procedure is strongly dependent on design ductility.

Keywords: Performance-Based Design; Displacement-Based Design accuracy; multi-span simply supported bridge RC piers; SDOF systems; equivalent viscous damping

1. Introduction

Displacement-based approaches, supplying approximate solutions for nonlinear structures, have gained a good reputation in the context of performance-based seismic design in recent years (Priestley 1993, 2000, Fajfar and Krawinkler 1997, Priestley *et al*. 2007, Ayala *et al*. 2012). Among these procedures, the most currently used one relies on the concept of equivalent linearization, initially developed by Shibata and Sozen (1976), and later implemented in the current form of direct displacement-based design (DDBD) method by Priestley *et al*. (Priestley 1993, Priestley *et al*. 2007, Sullivan *et al*. 2012). DDBD method requires use of an equivalent elastic structure (equivalent single degree of freedom, ESDOF) as a substitute for the real inelastic

---

∗Corresponding author, Ph.D. Student, E-mail: marco.dona@dicea.unipd.it
[a]Ph.D., E-mail: giovanni.tecchio@dicea.unipd.it
[b]Full Professor, E-mail: claudio.modena@unipd.it

systems of single (SDOF) or multi (MDOF) degree of freedom. The ESDOF structure is characterized by the effective stiffness K_{eff} (secant stiffness at maximum displacement Δ_u), the effective damping ξ_{eq}, related to the hysteretic energy absorbed, and the effective mass M_{eff}, which is the effective mass of the structure participating in the fundamental mode of vibration (see Fig. 1).

At present, DDBD method has reached a mostly complete degree of formalization with the recent publication of a Model Code for their adoption into seismic regulations (Sullivan *et al.* 2012). However, several aspects related to the method calibration are still under discussion. As for other simplified procedures, it is of interest to evaluate the representativeness of the equivalent linear SDOF systems in predicting nonlinear behavior of RC bridge structures (Grendene *et al.* 2012). Therefore, the attractiveness of the DDBD method may be considered as well for its conceptual coherency as for its accuracy against more refined nonlinear, time history analyses. The main sources of error of the method are the approximation of the substitute linear structure, characterized by the equivalent viscous damping, and the scaling of displacement elastic spectrum through the modification damping factor. It is of interest to evaluate the accuracy of the simplified DDBD method for a wide range of design cases, so that its attractiveness may be considered as well for its conceptual coherency as for the balancing of accuracy against reduced computational effort.

In this paper, the accuracy of the current DDBD procedure applied to simple SDOF systems is investigated with specific reference to multi-span, simply supported RC bridge piers. In the first part of the work, a parametric analysis is developed, comprising the design of a considerable amount of simple ideal oscillators with the current DDBD procedure and verified using dynamic inelastic time history analysis of the previously designed systems. A range of effective periods, T_{eff}, between 0.2 and 4.0 seconds are considered for ideal SDOF systems. Values of design displacement ductility, $\mu_\Delta{}^d$, between 1.25 and 5.0, are assumed to include possible low, medium, and high ductility behaviors. Four different equivalent viscous damping (EVD) models, ξ_{eq}, associated with three forms of R_ξ, scaling factor for the elastic displacement response spectrum (DRS), are evaluated. In total, 4212 ideal SDOF systems were designed and, subsequently, compared with the results obtained from nonlinear time history (NLTH) analyses performed for the same set of nonlinear simple oscillators based on Takeda Thin hysteretic model. The relative error of the DDBD method is thus obtained. By interpolating the medium error curves, a diagram of the expected approximation error of the simplified design method is subsequently derived.

In the second part of the work, a sensitivity study is performed to obtain realistic design values in terms of T_{eff} and $\mu_\Delta{}^d$ for cantilever RC piers with flexural behavior, all having different values of slenderness and reinforcement amount. The columns are designed for drift values, θ_d, between 1.5% and 4.0%. Using the medium error diagram, obtained previously, it is shown that, in the realistic design cases of RC bridge piers, the DDBD method offers good accuracy for low and medium ductility design levels ($\mu_\Delta{}^d<1.5$) while the relative error is higher for high values of displacement ductility ($1.5 \leq \mu_\Delta{}^d \leq 3.5$). Note that such high values are yet acceptable considering that the DDBD method generally overestimates.

Finally, an approximate relationship between ductility and drift is presented, since the definition of the admissible drift is an important aspect of the DDBD method, because it implies a certain value of ductility, the latter being adopted as a measure of the damage.
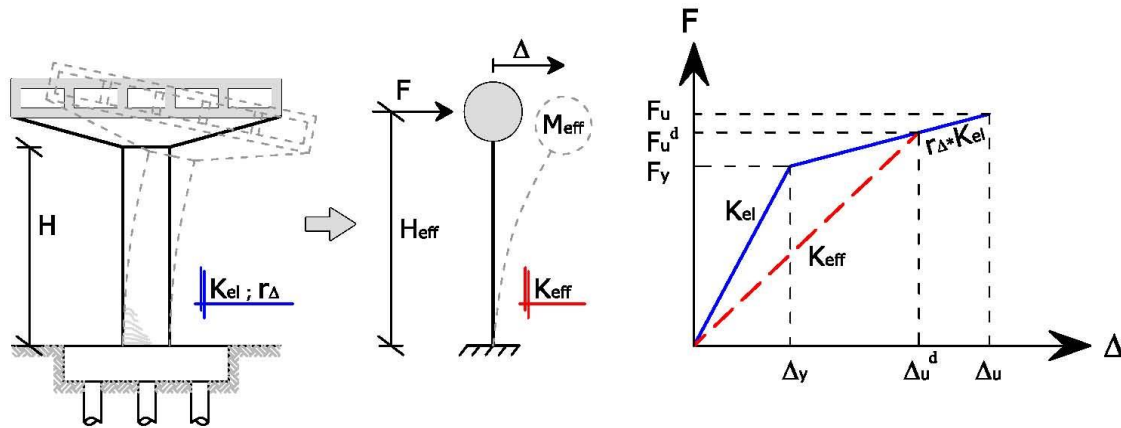
Fig. 1 Substitute structure for a cantilever bridge pier (SDOF system)

2. Error sources of the DDBD method for SDOF systems

One of the structures conforming more realistically to the assumptions of a SDOF approximation is a cantilever pier of a regular isostatic RC or PRC bridge under transverse excitation (Priestley *et al.* 2007). Its structural behavior under cyclic loads can be usually characterized by a simple oscillator, represented by a cantilever with a concentrated mass on the top. Thus, single bent cantilever piers are assumed as reference, realistic SDOF structures to be designed with the DDBD procedure and verified with NLTH analysis.

In order to assess the accuracy of the DDBD method when applied to simple inelastic SDOF systems, it is necessary to focus on the critical assumptions introduced by the procedure, as below:

1) equivalent linearization process with the estimation of an equivalent viscous damping, ξ_{eq};

2) use of over-damped displacement elastic spectra.

The equivalence of a simple nonlinear oscillator to an elastic system is based on the response of the system whose period T_{eff} is related to the secant stiffness at maximum displacement Δ_u of the nonlinear oscillator. The energy absorbed by the hysteretic steady-state cyclic response of the nonlinear oscillator is equated to ξ_{eq} of the linear oscillator, and maximum displacement responses of both systems are considered approximately equal. The appropriate calibration of the EVD model depends on the hysteresis cycles of the real system under seismic excitation, and represents the first source of approximation of the simplified design method.

Another source of uncertainty in the design process is created by the use of over-damped elastic displacement spectra to represent the peak response of inelastic ductile systems. Since the effective properties of ESDOF systems are elastic, the current DDBD method uses damped elastic response spectra for the design. Debate is yet ongoing over the correct formulation of the reduction factor, R_ξ. Alternative methods, such as the use of inelastic design spectra proposed by some authors (e.g., Chopra 2001), are not examined in this study.

Other important aspects of the current DDBD design procedure, relating to the initial choice of the target displacement and to the appropriate definition of 5% damped elastic displacement spectrum associated with the magnitude and fault plan distance (Faccioli and Villani 2009), are not herein considered.

3. Parametric analysis for ideal SDOF systems

3.1 Elastic displacement response spectrum

The seismic action for the design of SDOF systems is obtained from the elastic response spectrum proposed by EC8-2003 (CEN 2003). The horizontal component of "type 1" spectrum (5% damping) is selected as reference acceleration response spectrum for a ground of medium stiffness (type C, S=1.15, T_B=0.20 s, T_C=0.6 s, T_D=2.0 s) with PGA=0.35 g. The corresponding horizontal displacement response spectrum is derived from the following relation

$$S_\Delta(T) = S_a(T)\left[\frac{T}{2\pi}\right]^2 \tag{1}$$

where $S_\Delta(T)$ is the spectral elastic displacement response.

A set of seven synthetic accelerograms compatible with the EC8 spectrum is generated with the SIMQKE program (Gasparini and Vanmarcke 1976). The acceleration response spectra for the accelerograms compared with the code horizontal acceleration response spectrum and the code elastic displacement spectrum are plotted in Fig. 2.

3.2 Equivalent viscous damping models

The DDBD design procedure requires estimation of an equivalent viscous damping for the substitute linear structure. Damping relationships used in the parametric analysis consider the effect of ductility on damping, and are obtained in the form of a combination of elastic and hysteretic components (see Eq. (2))
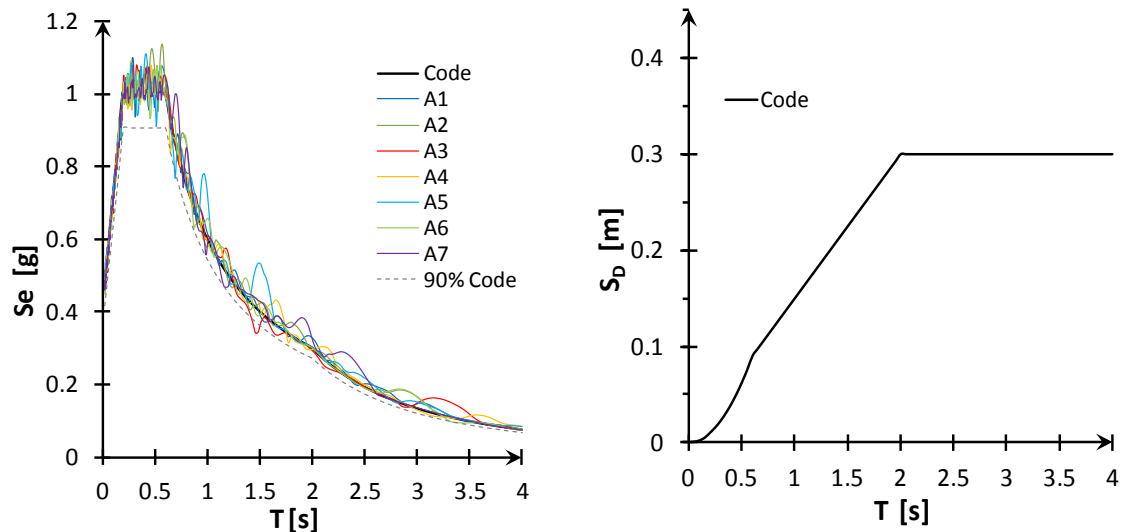
(a) Acceleration response spectra from time history set compared with code acceleration spectrum

(b) Code displacement elastic response spectrum, 5% damping

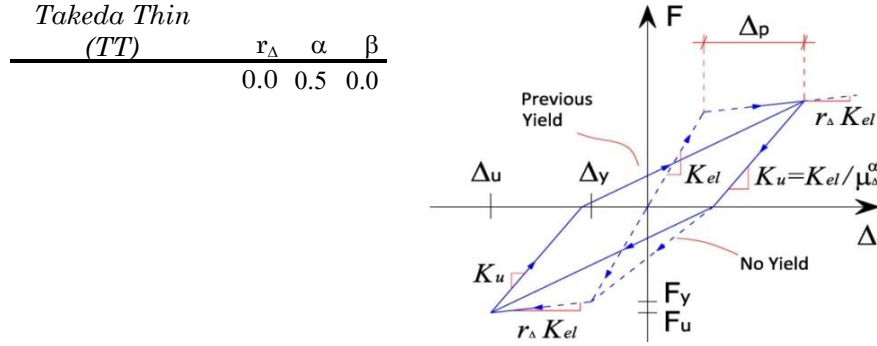Fig. 2 Acceleration and displacement response spectra: EC8-type1, $a_g = 0.35$, ground type C

Fig. 3 Parameters of Takeda Thin (TT) hysteretic model

$$\xi_{eq} = \xi_{el} + \xi_{hyst} \tag{2}$$

A value of $\xi_{el}=0.05$ is generally adopted for concrete structures, and ξ_{hyst} is calibrated taking into account the appropriate hysteresis rule for the structure to be designed.

In this case, Takeda Thin (TT) hysteretic model was used as a good representation of structural elements with significant axial load, such as bridge piers. An unloading stiffness factor of $\alpha=0.5$ and a bilinear stiffness ratio of $r_\Delta=0.0$ were adopted (see Fig. 3).

Four different EVD models, all calibrated for the TT hysteretic model, are compared in the numerical analyses with parameters r_Δ, α, and β taken as specified in Fig. 3. The first one, the *JDSS* model, is the original Jacobsen's model (Jacobsen 1930, 1960) tied to the initial stiffness of the nonlinear system. However, other expressions (*D.K.*, *G.B.P.*, *D.K.G.*) have been developed in the past years (Priestley 2005, Grant *et al.* 2005, Dwairi *et al.* 2007) more coherent with DDBD assumptions by relating the model to secant stiffness at peak response (this results in an equal period shift, T_{eff}/T_{el}, for all the considered hysteretic models).

The EVD expressions adopted in this study are reported in Eqs. (3)-(9):

a) *Jacobsen's Model (JDSS)* (Jacobsen 1930, 1960)

$$\xi_{eq} = \xi_{el} + \xi_{hyst} = \xi_{el} + \frac{2}{\pi}\left(1 - \frac{3}{4}\mu_\Delta^{\alpha-1}\gamma - \frac{1}{4}\right) \tag{3}$$

The expression can be simplified as follows with the values reported in Fig. 3

$$\xi_{eq} = \xi_{el} + \xi_{hyst} = \xi_{el} + \frac{1}{\pi}\left(1 - \frac{1}{\sqrt{\mu_\Delta}}\right)\% \tag{4}$$

b) *Model by Dwairi et al. (D.K.)* (Dwairi *et al.* 2007)

$$\xi_{eq} = \xi_{el} + \xi_{hyst} = \xi_{el} + C_{TT}\left(\frac{\mu_\Delta - 1}{\pi\mu_\Delta}\right)\% \tag{5}$$

where

$$C_{TT} = 50 + 40(1 - T_{eff}) \quad \text{for} \quad T_{eff} \leq 1s$$
$$C_{TT} = 50 \quad \text{for} \quad T_{eff} > 1s$$

(6)

c) ***Model by Grant et al. (G.B.P)*** (Grant *et al.* 2005)

$$\xi_{eq} = k\xi_{el} + \xi_{hyst} = k\xi_{el} + 0.215\left(1 - \frac{1}{\mu_\Delta^{0.642}}\right)\left[1 + \frac{1}{(T_{eff} + 0.824)^{6.444}}\right]\%$$

(7)

where

$$k = 1 \quad \text{for} \quad \mu_\Delta < 1$$
$$k = \mu_\Delta^\lambda \quad \text{for} \quad \mu_\Delta \geq 1$$

(8)

λ=0.340 for TT hysteresis rule and for the initial stiffness damping model.

The factor λ is the secant stiffness correction factor proposed by Grant *et al*. (Priestley 2005, Grant *et al.* 2005), and is related to the hysteresis rule selected (in this case, the TT hysteretic model). It introduces an adjustment that was proved to be necessary because in DDBD, the initial elastic damping is related to the secant stiffness at maximum displacement, whereas in inelastic time history analysis, it is conventional practice to relate the elastic damping to the initial stiffness. Without such an adjustment the verification of DDBD by NLTH analysis would be based on an incompatible assumption.

d) ***Model by Dwairi et al. with the correction factor for elastic damping (D.K.G.)*** (Priestley *et al.* 2007)

$$\xi_{eq} = k\xi_{el} + \xi_{hyst} = \mu_\Delta^\lambda \xi_{el} + C_{TT}\left(\frac{\mu_\Delta - 1}{\pi\mu_\Delta}\right)\%$$

(9)

where $C_{TT} = 50$, $k = \mu_\Delta^\lambda$ has the same value as in Eq. (8).

Eq. (9) modifies Eq. (5) introducing the correction factor for elastic damping, suggested by Grant et al. (Priestley 2005, Grant *et al.* 2005), with the same value of λ used in Eq. (8).

The (D.K.) and (G.B.P.) equivalent viscous damping models have a period dependency which leads to an evident increase of damping for T_{eff}<1 s, but is not significant for periods greater than 1.0 s in both cases. This dependency can be seen in Fig. 4(a) for various ductility levels. To compare different damping formulas only as functions of displacement ductility, the expressions for (D.K.) and (G.B.P.) models have been plotted for T_{eff}≥1 s and T_{eff}=4 s, respectively in Fig. 4(b). Firstly, it can be observed that a significant difference is presented by the (D.K.) model, due to the absence of the correction factor $k=\mu_\Delta^\lambda$ for the elastic damping, which leads to an increase in the underestimation of the damping ratio for an increase in the ductility level. Moreover, the highest damping values are given by the JDSS model, which represents a sort of upper envelope even if it does not include a correction factor for elastic damping. High level of overestimation of JDSS model has been proved by previous authors (Chopra 2001, Dwairi *et al.* 2007). In this specific
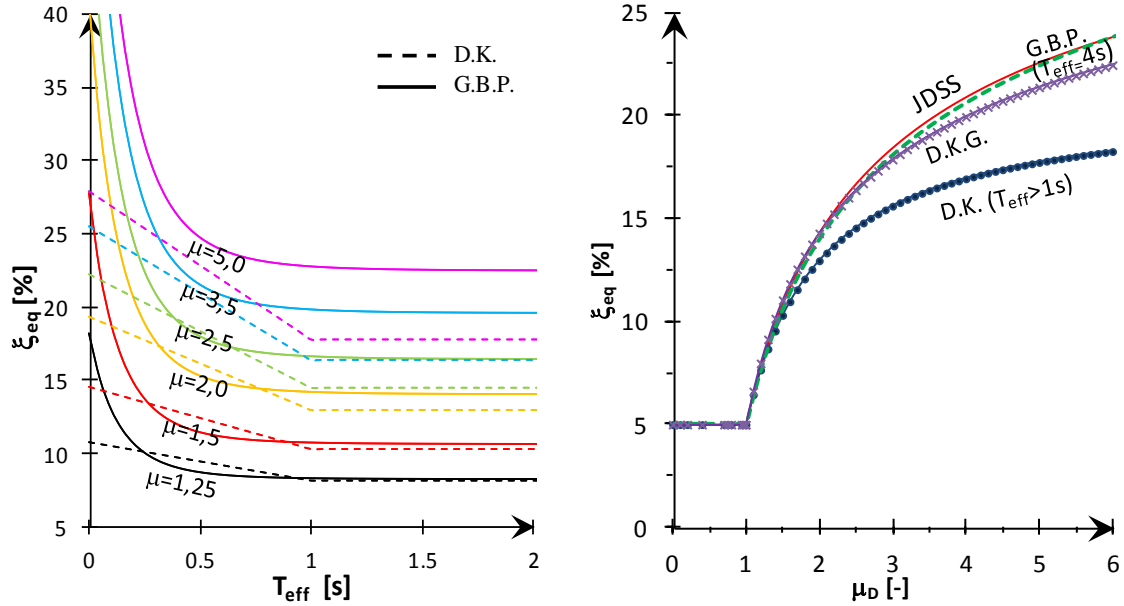
(a) Period dependency of EVD models (D.K.) and (G.B.P.)

(b) ξ_{eq} values for models (JDSS), (D.K.) for $T_{eff}>1$ s, (G.B.P.) for $T_{eff}=4$ s and (D.K.G.)

Fig. 4 Period dependency of hysteretic component for EVD models (D.K.) and (G.B.P.), plotted for different ductility levels, and equivalent viscous damping ratio provided by the four models based on the TT hysteretic rule

case, being the TT hysteresis rule associated with the JDSS model, its trend seems to be very close to those of more "advanced" models like (G.B.P) and (D.K.G.). Thus, the scatter in the results is expected to be lower than that in other cases in which "fatter" hysteretic models are adopted (for example, the Takeda Fat or the Elastoplastic model).

3.3 Response spectrum reduction factors

The basic elastic displacement response spectrum (relative to an elastic damping ratio of $\xi_{eq}=0.05$) shall be damped with regard to the calculated structural equivalent viscous damping, ξ_{eq}, by multiplying spectral ordinates by the reduction factor, R_ξ

$$S_{\Delta\xi}(T) = R_\xi S_{\Delta 0.05}(T) \qquad (10)$$

To date, seismologists are still debating about the appropriate form of damping modifier, R_ξ, for elastic spectral displacement. In this study, three commonly used expressions are compared. The first being Eq. (11) which was proposed by Newmark and Hall (1982). The second one is Eq. (12), presented in the 1998 edition of Eurocode 8 (CEN 1998) which was subsequently replaced by the third expression, Eq. (13), in the 2003 revision of EC8 (CEN 2003).

a) ***Newmark and Hall (NH)*** (Newmark and Hall 1982)

$$R_\xi = [1.31 - 0.191\ln(100\xi)] \tag{11}$$

b) **EC8-1998** (CEN 1998)

$$R_\xi = [0.07/(0.02 + \xi)]^{0.5} \tag{12}$$

c) **EC8-2003** (CEN 2003)

$$R_\xi = [0.10/(0.05 + \xi)]^{0.5} \tag{13}$$

Other expressions for R_ξ have been recently proposed by some authors (Faccioli and Villani 2009) for near-field sites. Such effects on spectral displacements are not addressed in this study.

3.4 Evaluation algorithm

The parametric analysis was performed with the aim of comparing the DDBD target displacements to the relative peak displacements from the time history (TH) response for a wide range of SDOF systems. The analysis is based primarily on the definition of a series of simple nonlinear oscillators, obtained by "inverting" the current DDBD procedure.

A set of initial input parameters, in terms of T_{eff} and $\mu_\Delta{}^d$, is chosen to address the design, and the EVD model is selected (Eqs. (3)-(9)). The over-damped displacement spectra can be subsequently determined by scaling the elastic spectrum with the reduction factor, R_ξ, and the design displacement, $\Delta_u{}^d$, calculated by entering the damped spectra with the input parameter effective period, T_{eff}. Then, the capacity curve for each ideal oscillator is finally derived on the basis of pre-fixed design ductility, $\mu_\Delta{}^d$, and design displacement, $\Delta_u{}^d$, calculated previously.

At this point, the design of the ideal SDOF system can be considered complete. Once the key features of each nonlinear SDOF system have been defined by means of the capacity curve, and the hysteresis rule is associated (Takeda Thin model, Fig. 3), the inelastic response in terms of ultimate displacements can be evaluated using nonlinear analysis in the time domain, and the relative error, compared to the DDBD design displacement, can be estimated.

The evaluation procedure (Fig. 5) consists of the following steps:

(I) Define initial input parameters
a) Select the basic response spectrum, $S_{\Delta 0.05}(T)$.
b) Select a value for design displacement ductility, $\mu_\Delta{}^d$, and effective period, T_{eff}, of the ideal SDOF oscillator.

(II) Determine the damped response spectrum
c) Calculate the equivalent viscous damping, ξ_{eq}, as a function of ductility, using one of the models given by Eqs. (3)-(9).
d) Obtain the response spectrum reduction factor, R_ξ, using one of the Eqs. (11)-(13).
e) Multiply the basic response spectral ordinates by the reduction factor, R_ξ, and obtain the design displacement response spectrum, $S_{\Delta\xi}(T)$, in accordance with Eq. (10).

(III) Calculate the target response
f) Enter the damped displacement spectrum, $S_{\Delta\xi}(T)$, with $T_{eff,}$ and calculate the target displacement, $\Delta_u{}^d$.
g) Calculate the design acceleration, $a_u{}^d$, entering the acceleration response spectrum, $S_{a\xi}(T)$, with T_{eff}.

(IV) Obtain the capacity curve for SDOF oscillator
h) Calculate the yield displacement, Δ_y, for the SDOF system as $\mu_\Delta^d = \Delta_u^d / \Delta_y$.
i) Calculate the elastic period using the following equation

$$T_{el} = T_{eff}\sqrt{\left(1 + r_\Delta \mu_\Delta^d - r_\Delta\right)/\mu_\Delta^d} \tag{14}$$

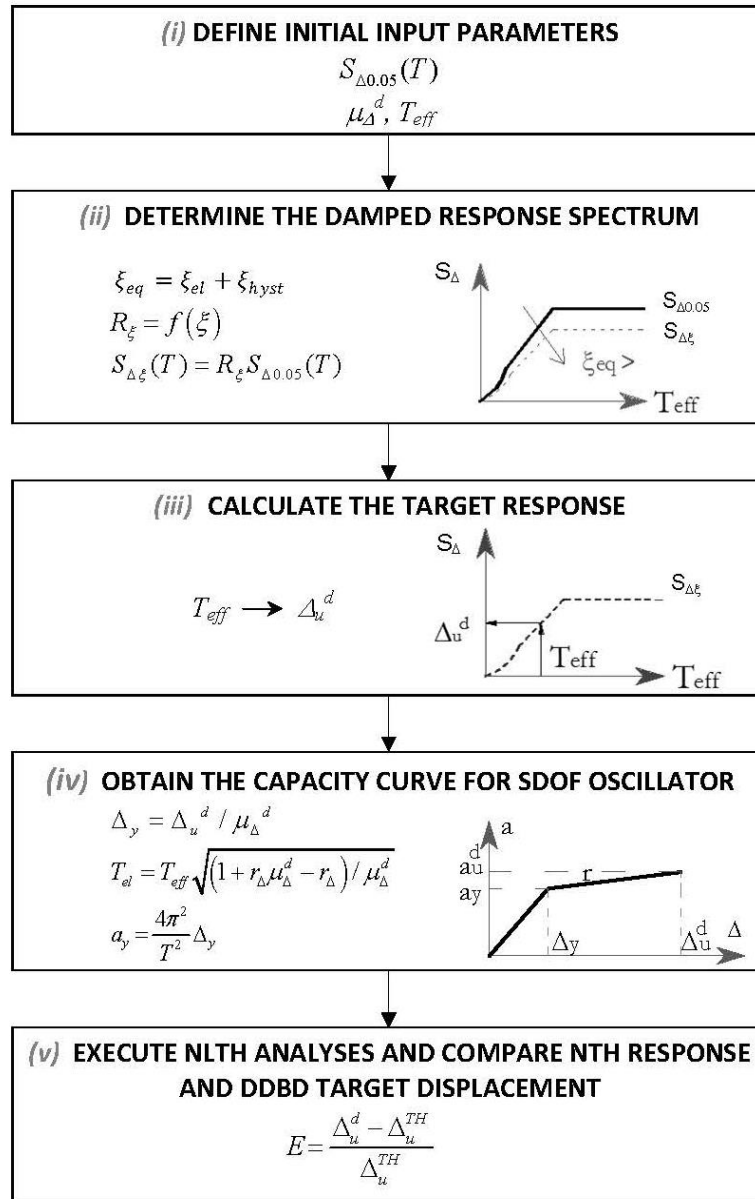where r_Δ is the bilinear stiffness ratio in Fig. 1.

Fig. 5 Flowchart of the evaluation algorithm used in the parametric analysis

l) Calculate the yield acceleration as

$$a_y = \frac{4\pi^2}{T_{el}^2}\Delta_y \tag{15}$$

The capacity curve has thus been obtained and can be plotted in the acceleration-displacement (A-D) plane.

(V) Execute NLTH analyses
m) Run the TH analyses using the nonlinear SDOF system defined by the capacity curve and adopting the Takeda Thin hysteretic model (with the parameters specified in Fig. 3). The value ξ_{el}=5% is to be assumed for the elastic viscous damping.

(VI) Compare NLTH response and DDBD target displacement
n) Plot the displacement, Δ_u^{TH}, obtained as the average of maximum displacement demands calculated for the seven time histories, compatible with the design spectrum and represented in Fig. 2. Afterwards, compute the relative error

$$E[\%] = \frac{\Delta_u^d - \Delta_u^{TH}}{\Delta_u^{TH}} \tag{16}$$

Following the procedure described from point (I) to (VI), a parametric study was carried out by considering 39 different values of effective period, T_{eff}, as input parameters and defined between 0.2 s and 4 s, at 0.1 s intervals, and nine different ductility levels, μ_Δ^d, in the range 1.25-5. Consequently, 351 analyses were performed for a single design spectrum. Each spectrum was obtained via scaling the basic response spectrum after choosing from among four types of equivalent damping models, ξ_{eq} (Eqs. (3)-(9)), associated with three different scaling factors, R_ξ (Eqs. (11)-(13)). In total, 4212 nonlinear SDOF systems were designed, and subsequently, verified in terms of displacement demands through dynamic nonlinear analyses in the time domain.

3.5 DDBD verification

In this section, a synthesis of the results obtained from the parametric analyses on ideal SDOF systems is reported. Figs. 6-7 show comparison of the results for different EVD models and a pre-fixed form of the damping modification factor, R_ξ. The single case of R_ξ=EC8-2003 is reported, but the following considerations are also based on similar results obtained for other R_ξ formulae, NH and EC8-1998. The relative errors between the design displacement of the DDBD method and the mean value of the TH peak displacements are represented for constant displacement ductility values, μ_Δ^d.

It is apparent that, for all EVD models, overestimation errors increase with high ductility values. This seems reasonable that, prediction of a "near" elastic response is more easily reproduced by a linearized system than an inelastic behavior requiring a deep excursion into the plastic field.

Problems related to the overestimation errors of JDSS model are not as evident as they are in other studies. This is due to the shape of the adopted hysteretic model (Takeda Thin model) for the nonlinear cyclic behavior of bridge piers, as already anticipated.

The graphs show that, three of the different evaluated EVD models give very similar results for T_{eff}>0.75 s, and consequently, the same trend of the relative error plot is obtained for this range of

T_{eff}. The exception is represented by the (D.K.) model, exhibiting the greatest inaccuracy for $T_{eff}>0.75$ s, due to the absence of an elastic damping correction.

For $T_{eff}<0.75$ s, JDSS and (D.K.G.) models sensibly underestimate the EVD required to the linear SDOF system to equate the nonlinear peak displacements obtained with TH analyses.

This is due to the absence of a dependence on the effective period, T_{eff}, which, on the contrary, is accounted for by (D.K.) and (G.B.P.) models. In particular, the best results are obtained for all ductility levels by (G.B.P.) model, even if it is not accurate in the low-period range.
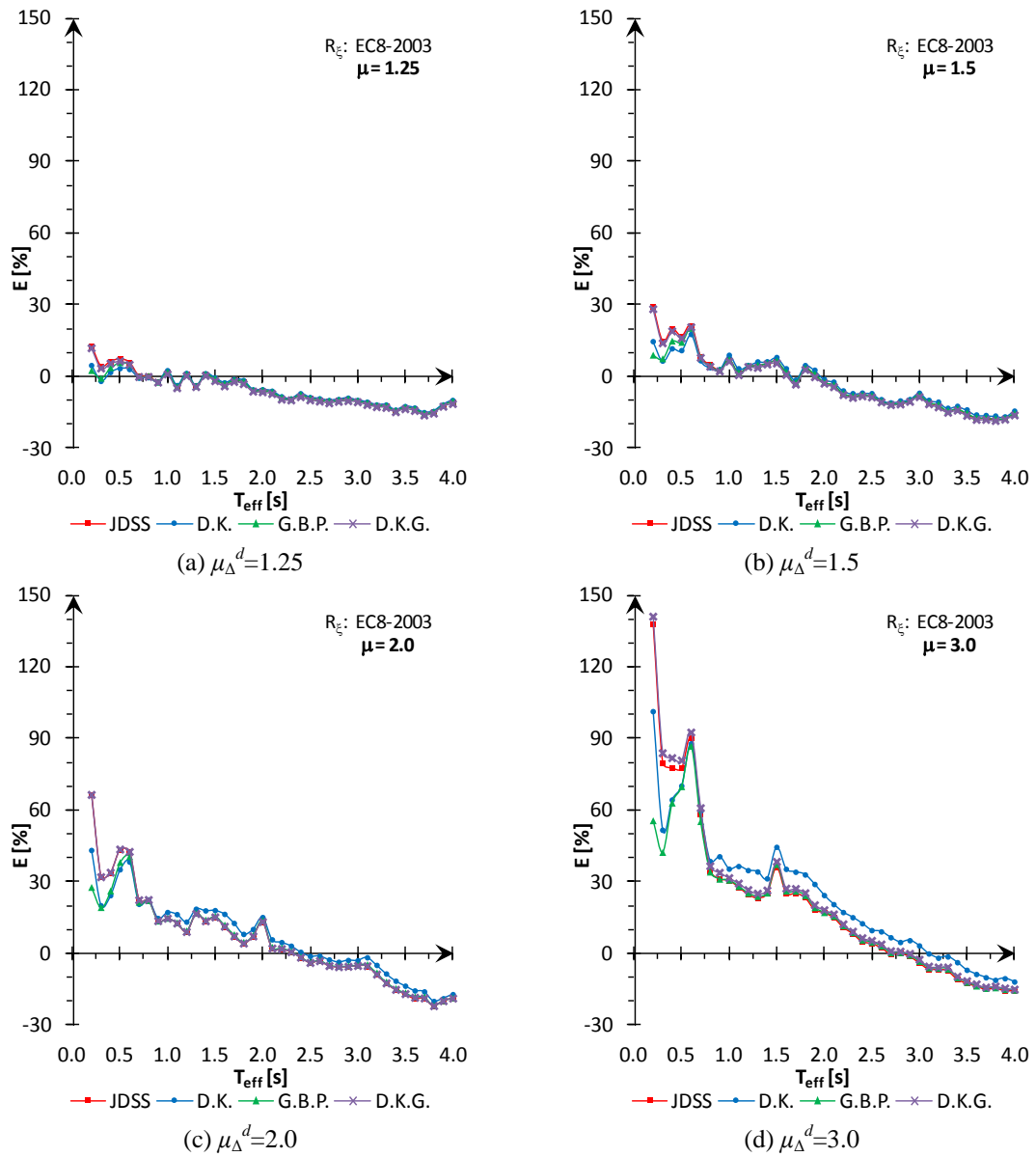

Fig. 6 Relative error obtained (Eq. (16)) using different EVD models and a pre-fixed spectrum reduction factor, R_ς=EC8-2003

Finally, it can be observed that, it will be unusual for normal structures (wall and frame buildings or bridges) to have effective period values less than 0.75-1 s, and this is confirmed also by the results of the sensitivity analysis on realistic pier designs developed in the second part of the work.

Since T_{eff} is greater than 1 s in most of real design cases, and since the (D.K.G.) model requires the ductility value, $\mu_\Delta^{\,d}$, as the only input data (unlike the G.B.P. model that also needs T_{eff}, an output of the DDBD method, leading to an iterative procedure), it can be concluded that, the (D.K.G.) model is effectively the most convenient one.

In Figs. 8-9, the comparison of relative errors obtained in the design displacement prediction using different forms for the spectral reduction factor, R_ξ, is presented. The same equivalent damping model (D.K.G.) is used in these cases with reference to some pre-fixed ductility levels, $\mu_\Delta^{\,d}$=1.25, 1.5, 2.0, 3.0, 4.0, and 5.0. It can be observed that accuracy diminishes with the increase of the ductility demand for all the R_ξ forms.

The formula leading to more conservative results (greatest overestimation errors) is Newmark-Hall's, which results to be too cautious. As for the other two, *EC8-2003* and *EC8-1998*, an overall reduction in the relative error can be observed as the period increases with a quite comparable trend for T_{eff}>1 s. The most precise equivalent spectral elastic displacement seems to be
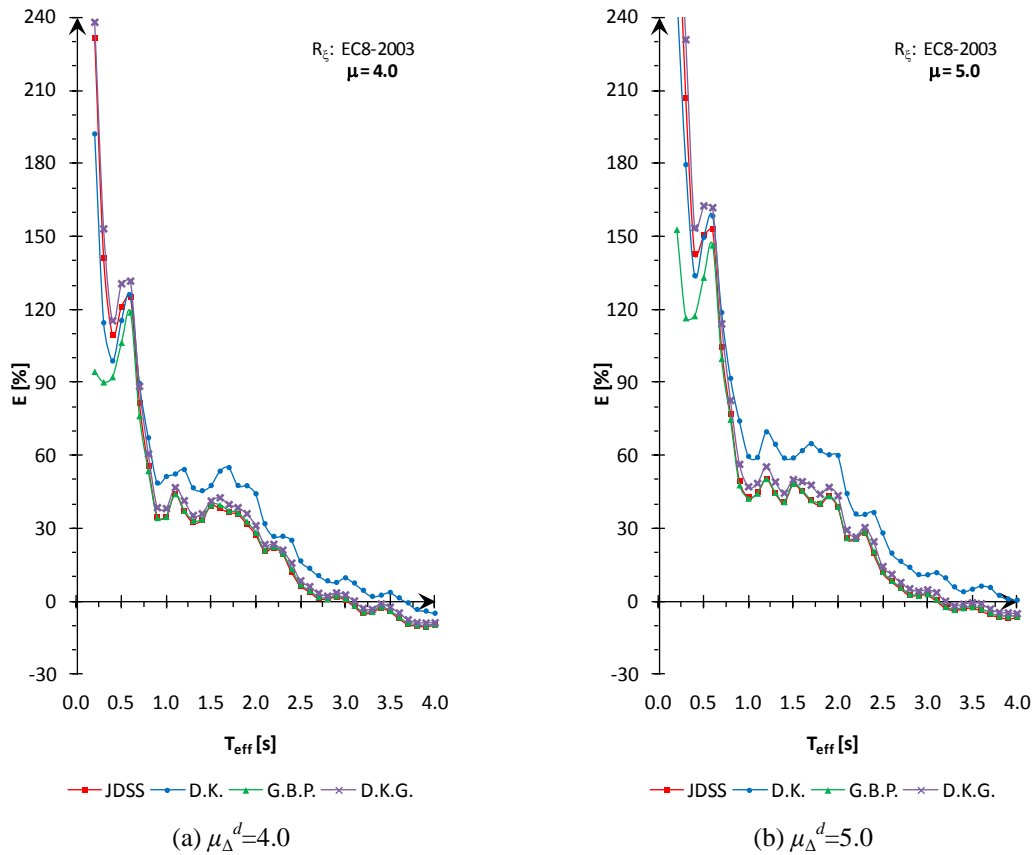

(a) $\mu_\Delta^{\,d}$=4.0   (b) $\mu_\Delta^{\,d}$=5.0

Fig. 7 Relative error obtained (Eq. (16)) using different EVD models and a pre-fixed spectrum reduction factor, R_ξ=EC8-2003
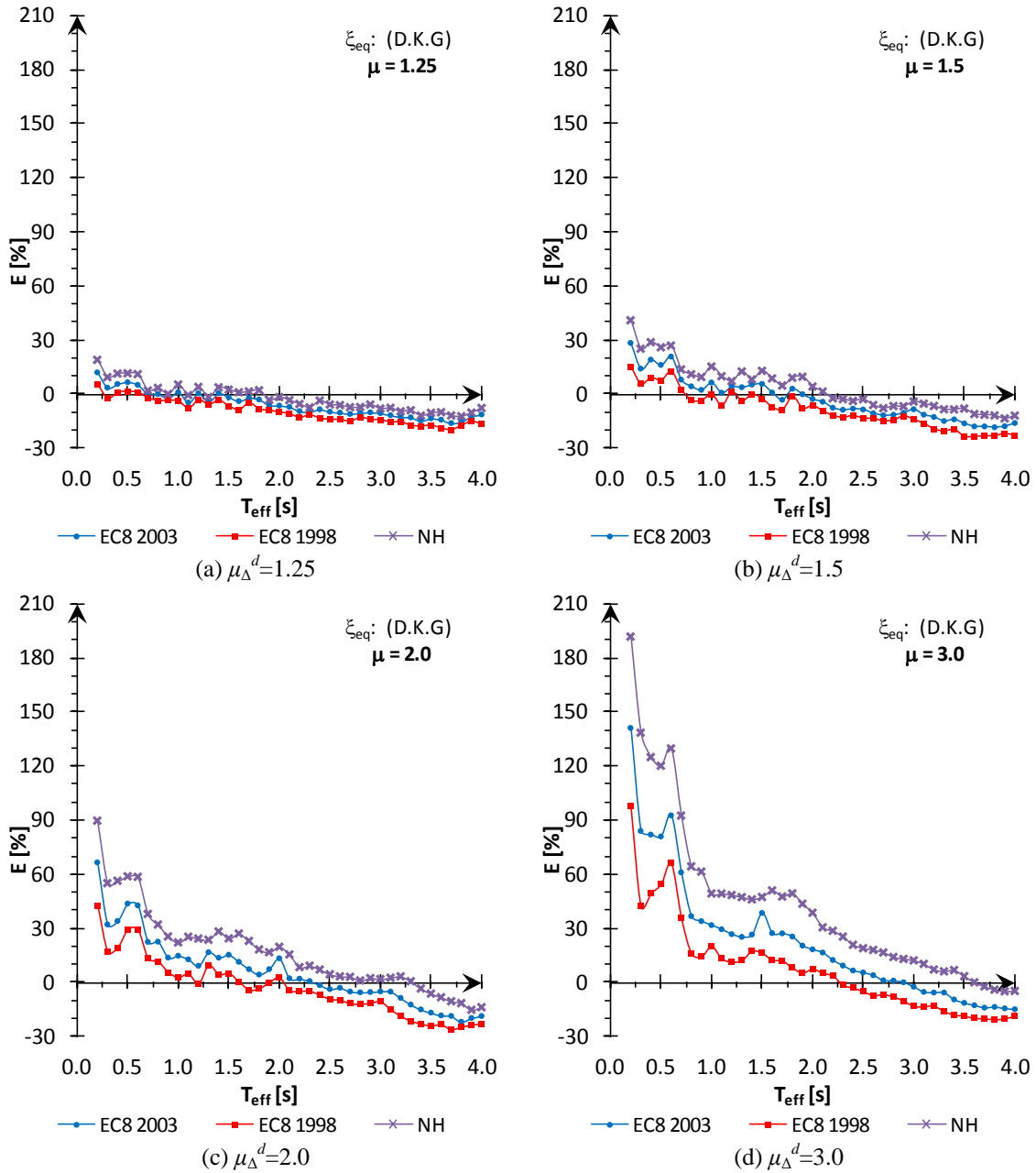
Fig. 8 Relative error obtained (Eq. (16)) using different expressions for the spectrum reduction factor, R_ς, and a pre-fixed EVD model, ξ_{eq}=(D.K.G.)

obtainable using the R_ς=*EC8-1998* but the *EC8-2003* curve remains steadily above the corresponding *EC8-1998* curve. Therefore, the underestimation error is smaller for T_{eff}>2 s. Such consideration can justify the preference for the *EC8-2003* formula currently adopted by Sullivan *et al.* (2012).

The results obtained for the other damping models and ductility levels are not reported here for brevity, but same conclusions can be drawn.

Following the verification process described by the flowchart in Fig. 5, it is possible to plot the iso-ductility displacement design spectra, and compare them with the inelastic displacement spectra obtained by NLTH analysis. An example of this comparison is given in Fig. 10 for the choice of the EVD model based on (*D.K.G.*) and of the scaling factor given in *EC8-2003*. In Fig. 11, the relative error according to Eq. (16) is plotted with the same assumptions for the entire period range, considering all the different ductility levels.

In Fig. 10, it can be observed that the DDBD target displacements, corresponding to the inelastic displacement response spectra, are generally higher than the TH average peak displacement demands, at least up to the corner point of the spectra. As the displacement that results from the nonlinear analysis of bridges is smaller, it can be deduced that the method tends to overestimate the response.

The point of intersection between the DDBD design displacement spectrum and the curve of the effective peak displacement demand (obtained from TH analysis for the nonlinear SDOF system) shifts towards higher values of T_{eff} by increasing ductility level. This means that the overestimation error of the DDBD method increases with increase in μ_Δ^d values; thus, the method is proved to be more conservative for high-ductility design cases.

The method is generally conservative, at least for structures with $T_{eff}<2.5$-3.0 s.

Overestimation errors, for ideal SDOF oscillators, are significantly dependent on the design ductility level, while underestimation errors are of small relevance.

As previously noted, it should be underlined that, the effective periods smaller than 0.7 s do not apply to the design of real piers of flexural behavior (see also subsequent Figs. 13-14).
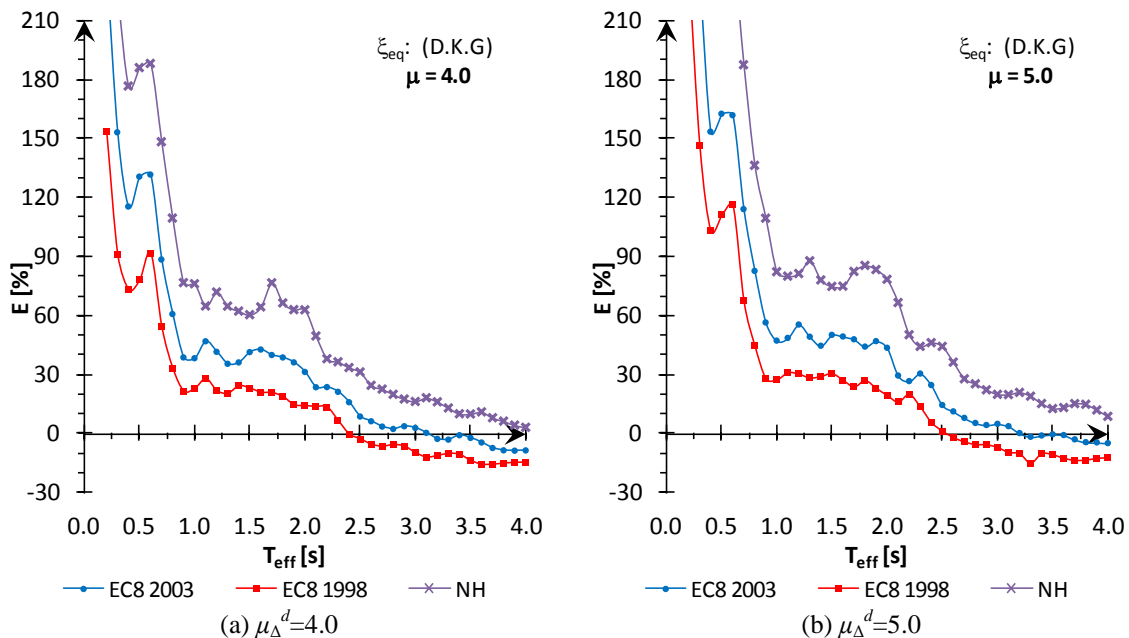

(a) $\mu_\Delta^d=4.0$ (b) $\mu_\Delta^d=5.0$

Fig. 9 Relative error obtained (Eq. (16)) using different expressions for the spectrum reduction factor, R_ξ, and a pre-fixed EVD model, ξ_{eq}=(D.K.G.)
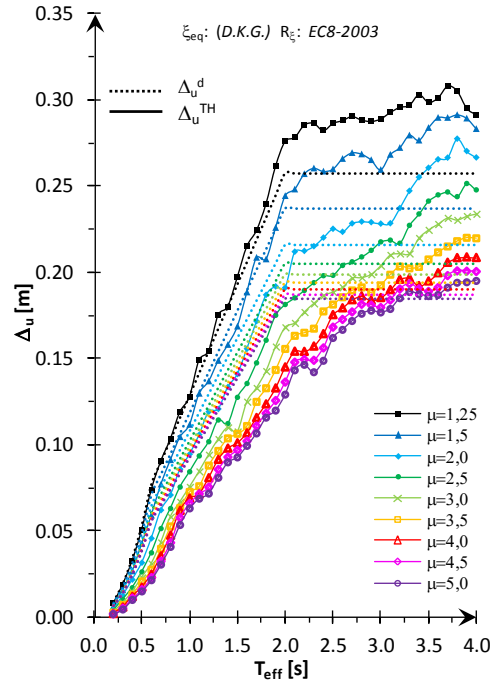
Fig. 10 Design displacements, Δ_u^d, of the DDBD method compared with the average inelastic displacement spectra obtained by TH analyses, following the procedure in Fig. 5, for all ductility levels (μ_Δ^d=1.25-5.0). Case study: ξ_{eq}=(D.K.G.), R_ξ=EC8-2003
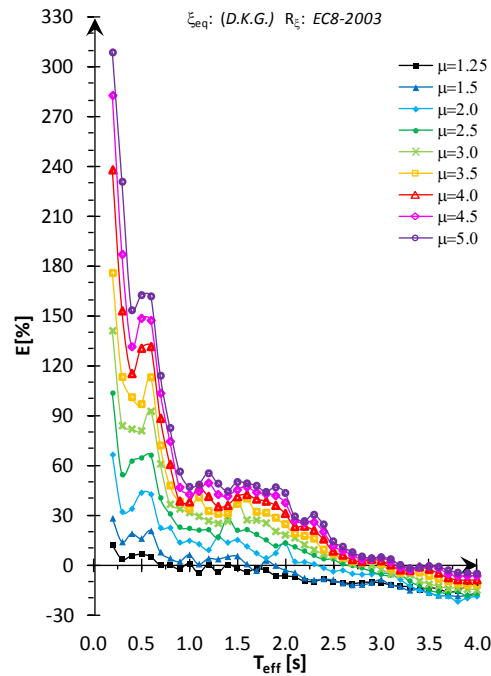

Fig. 11 Relative error obtained for design displacements, Δ_u^d, in Fig. 10 with the average inelastic displacement spectra obtained by TH analyses. Case study: ξ_{eq}=(D.K.G.), R_ξ=EC8-2003

Thus, the high errors resulted in simplified DDBD method in this range are of small significance and no practical interest.

It will be useful to know the accuracy of the DDBD method when applied to SDOF systems.

The error is introduced by the simplified procedure due to the approximations of a substitute linear structure characterized by the equivalent viscous damping, ξ_{eq}, and the scaling of the displacement elastic spectrum through the modification damping factor, R_ξ. With this aim, a diagram of the mean relative error is plotted in Fig. 12. A polynomial interpolation of the relative error curves plotted in Fig. 11 for constant ductility levels is obtained, and the average prediction error is expressed as a function of design displacement ductility, μ_Δ^d, (which is an input of the DDBD method) and T_{eff}.

The error ranges identified in Fig. 12 define the design areas in which all the possible SDOF systems designed with the simplified DDBD method are affected by medium errors within the extreme values of the range.

4. Error prediction for Direct Displacement-Based Design of cantilever RC bridge piers

This section deals with a sensitivity analysis on realistic SDOF structures, namely cantilever RC piers of simply supported bridges. The study was carried out with the aim of identifying the ranges of all possible combinations of displacement ductility, μ_Δ^d, and effective period, T_{eff}, for such structures.

4.1 Input data and design limitations

The input data for the sensitivity analysis are listed below.

- *Seismic action:* the reference elastic spectrum is the same as the one used for the parametric analysis in the first part of the work, i.e., EC8-2003 spectrum "type 1", Ground type C (S=1.15, T_B=0.20 s, T_C=0.6 s, T_D=2.0 s), a_g=0.35 g, and 5% damping.

- *Effective mass* of the SDOF system: two values of tributary mass are considered, M_{1eff}=250 t; M_{2eff}=500 t.

- *Materials:* effective properties are used for concrete and reinforcement. Concrete C32/40: f'_{ce}=1.3 * f'_c=43.2 MPa. Reinforcement steel B450C: f_{ye}=1.1 * f_y=495 MPa.

- *Pier geometry, bar diameter:* circular section, concrete cover of 3.5 cm, and bar diameter d_{bl}=30 mm.

The following limits relating to the geometry of piers (diameter, D, and height, H), normalized axial load, v, slenderness, λ, and reinforcement ratio, ρ_l, are introduced to address the design of circular cantilever piers for typical multi-span simply supported girder bridges.

a) Geometric parameters (to individuate an appropriate geometric range of sections for RC bridge piers and guarantee a flexural behavior)

$$D \geq 1m \qquad \text{(minimum diameter)} \tag{17}$$

$$H/D \geq 3.5 \quad \text{(minimum height /diameter ratio)} \tag{18}$$

b) Maximum value of the dimensionless axial load
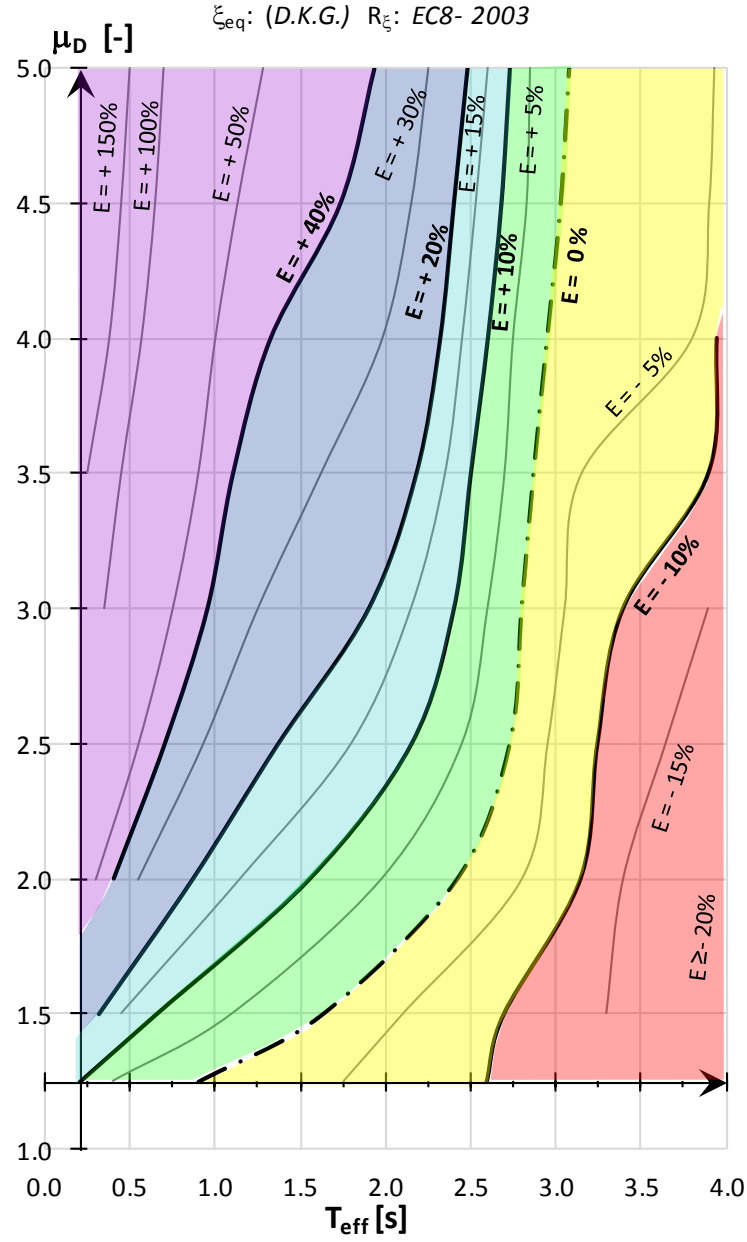
$$v = N_{Ed}/\left(f'_c A_c\right) < 0.6 \tag{19}$$

Fig. 12 Relative error ranges (%) for the SDOF systems designed with the DDBD method. Case study: ξ_{eq}=(D.K.G.), R_ξ=EC8-2003

c) Pier slenderness (limit suggested by NTC'08, for linear analysis)

$$\lambda < \lambda_{\lim} = 15.4 \frac{C}{\sqrt{\nu}}$$

(20)

where the coefficient *C* is expressed by $C=1.7-r_m$, with the limits $0.7 \leq C \leq 2.7$ depending on the first order distribution of flexural moments at the pier top and bottom $r_m = M_{01}/M_{02}$ (set equal to 0 for a cantilever pier).

d) Longitudinal reinforcement ratio

$$0.5\% \leq \rho_l \leq 4\% \tag{21}$$

Adequate confinement and sufficient transverse reinforcement are supposed to be used, ensuring ductile flexural response of the piers.

4.2 Design process of cantilever RC piers and limits check

A series of circular cantilever columns are designed with the DDBD method, considering target design drift limits $\theta_d=0.015-0.04$, and stepping 0.005 (six values). Nine levels of design displacement ductility are addressed: $\mu_\Delta^d=1.25$, 1.5, 2.0, 2.5, 3.0, 3.5, 4.0, 4.5, and 5.0.

The realistic design limits fixed above in terms of slenderness, amount of reinforcement, and height/diameter ratio are implemented. Design cases not satisfying the previous limits are considered "unrealistic" and are excluded from the number of possible solutions.

Numerical analyses are carried out by considering an equivalent viscous damping given in (D.K.G.) model (Eq. (9)), and the spectrum reduction factor supplied by the *EC8-2003* formula (Eq. (13)).

The design procedure consists of the following steps:

a) Initial input: effective mass value, M_{eff}, is chosen; target drift level $\theta_d=0.015-0.04$ is selected from amongst six prefixed values; displacement ductility level, μ_Δ^d, is chosen.

b) Damped displacement response spectrum is constructed using Eqs. (10) and (13).

c) T_{eff} for the selected μ_Δ^d and θ_d values is chosen (the same period range of 0.2-4.0 s used in the parametric analysis of ideal SDOF systems was considered).

d) The damped displacement spectrum $S_{\Delta\xi}(T)$ is entered with T_{eff}, and the target displacement Δ_u^d is calculated.

e) The yield displacement is obtained as

$$\Delta_y = \Delta_d \big/ \mu_\Delta^d \tag{22}$$

f) The pier height is estimated with the relation

$$H = \Delta_u^d \big/ \vartheta_d \tag{23}$$

g) The yield curvature Φ_y is calculated, the strain penetration length L_{sp} being known

$$L_{sp} = 0.022 f_{ye} d_{bl} \tag{24}$$

$$\Phi_y = 3\Delta_y \big/ \left(H + L_{sp}\right)^2 \tag{25}$$

h) The pier design diameter is determined using a simplified relation for dimensionless yield curvature Φ_y (Priestley 1993)

$$\Phi_y = 2.25\varepsilon_y / D \quad \rightarrow \quad D = 2.25\varepsilon_y / \Phi_y \tag{26}$$

i) First design check is done for minimum diameter requirement and expected flexural behavior, according to Eqs. (17)-(19). If the limits are not satisfied, the design case is excluded as possible realistic solution, and the process is interrupted.

j) Second design check is done for pier slenderness, λ, according to Eq. (20). If the limit is not respected, the procedure is stopped.

k) If requirements of steps *i* and *j* are satisfied, the effective stiffness, K_{eff}, is calculated as

$$K_{eff} = 4\pi^2 M_{eff} / T_{eff}^2 \tag{27}$$

l) Design shear (including *P-Δ* effects), F_u^d, and bending moment at the pier base, M_{base}, are determined

$$F_u^d = K_{eff} \Delta_d + 0.5 P \Delta_d / H \tag{28}$$

$$M_{base} = F_u^d H \tag{29}$$

m) Minimum longitudinal reinforcement is determined. For the calculated M_{base} and acting axial load, ν, the minimum reinforcement ratio is computed for symmetric reinforcement, imposing strain limits of ε_c=0.004 and ε_s=0.015. Reinforcement ratio percentages according to Eq. (21) are accepted only.

The research of the realistic design cases was carried out by determining the extreme values of the effective period admissible range, $T_{eff,\min}$ and $T_{eff,\max}$, for a pre-fixed drift, θ_d, and an established ductility level, μ_Δ^d.

In Figs. 13-14, the realistic designs obtained are plotted for the case of tributary mass M_{eff}. For a better graphic result, the occurrences corresponding to single designs are represented with a range of T_{eff} at 0.1-0.15 s. The design ductility values, μ_Δ^d, are plotted versus effective period, T_{eff}, and the obtained ranges for pier slenderness, λ, are superimposed.

It is understood that typical design values for RC cantilever piers are obtained for a range of μ_Δ^d=1.25-5.0, and effective periods vary from a minimum of 0.75 s to almost 3.0 s. The values of considered slenderness, λ, vary from 28 to 69.

In order to better compare the final results obtained with target ductility values commonly accepted in Europe for bridge design, it seems appropriate to consider the range of the parameter μ_Δ^d according to the maximum values of behavior factors, *q*, currently proposed by seismic codes (EC8-2003, NTC '08) for reinforced concrete pier design (implicitly assuming the validity of the "equal displacement" rule, $q=\mu_\Delta^d$ for the typical range of periods considered). Two classes were defined: low-medium design ductility (DCM) when $1.25 \leq \mu_\Delta^d < 2.0$, and high design ductility (DCH) when $2.0 \leq \mu_\Delta^d \leq 3.5$.

A final plot superimposing the "realistic" design points to the medium error diagram, previously obtained in the (T_{eff}, μ_Δ^d) plane, (see Fig. 15) is proposed; thus, it is possible to derive directly the error prediction of the DDBD method when applied to the design of cantilever piers of simply supported RC bridges (SDOF systems).

It can be observed that the DDBD method is generally conservative. Underestimation errors are limited for any realistic design almost always less than 10% with few cases (6%) with just slightly higher relative errors (E_m<12%).

As already seen for ideal SDOF systems, the accuracy of the DDBD method, described as overestimation error range, is dependent on design ductility:
- for low-medium ductility design cases ($\mu_\Delta^d \leq 1.5$), the DDBD method is yet very accurate, with

a low error range calculated for the single pier design, $E_m<+10\%$;

- for high ductility values ($1.5<\mu_\Delta^d\leq3.5$), the relative errors are higher, even if most of the samples attain error levels that can be still considered as acceptable ($E_m<+20\%$ in 63%, and $E_m<+30\%$ in 90% of the design cases), taking into account that the error is an overestimation inaccuracy, and that the design process is a simplified direct method. Nevertheless, there is a non-negligible percentage of structures (10%) with higher errors but a maximum below 40%.
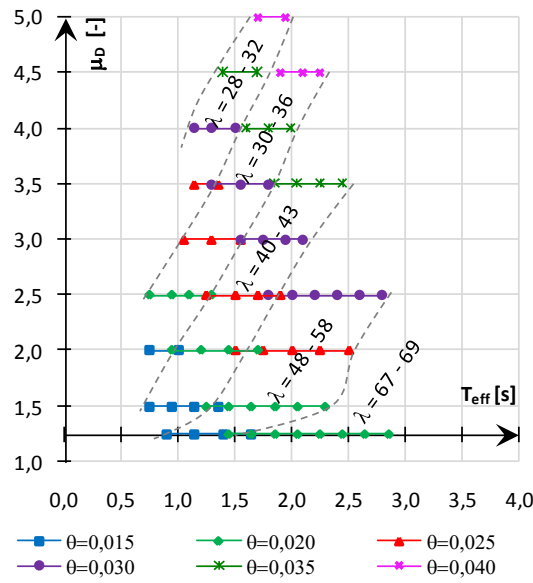
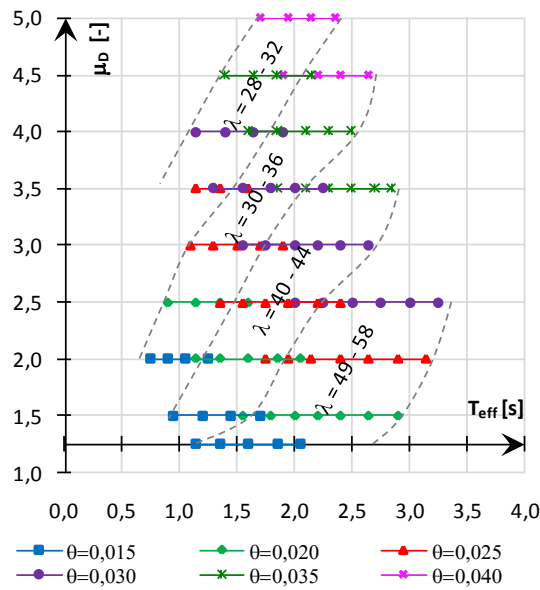Fig. 13 Realistic SDOF designs obtained for cantilever RC piers with tributary mass M_{eff}=250 t

Fig. 14 Realistic SDOF designs obtained for cantilever RC piers with tributary mass M_{eff}=500 t
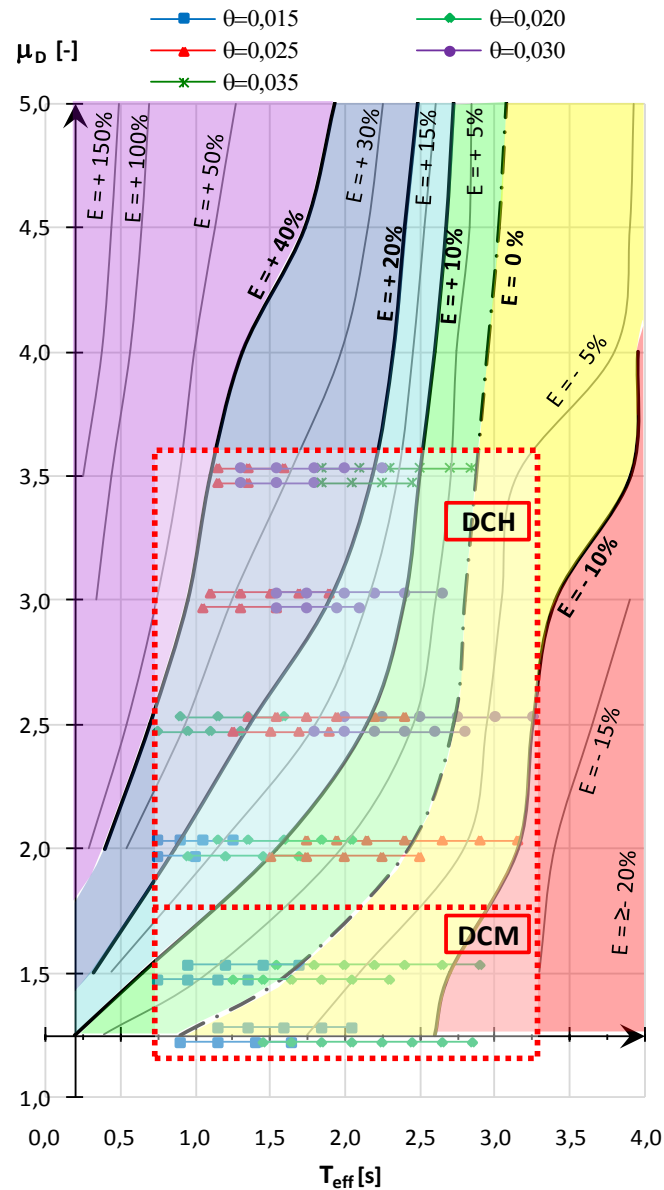
Fig. 15 Relative error prediction (%) for the DDBD method applied to the design of cantilever RC bridge piers (SDOF systems). The medium error diagram in the background refers to Fig. 12, while the design points for realistic cases are extracted from Figs. 13-14

4.3 Relationship between drift and ductility

It could be of interest to estimate directly the expected accuracy of the DDBD method in relation to the choice of the design drift level, θ.

A direct relationship between drift and ductility allows to use the medium error diagram supplied in Fig. 15, once the performance drift level is fixed.
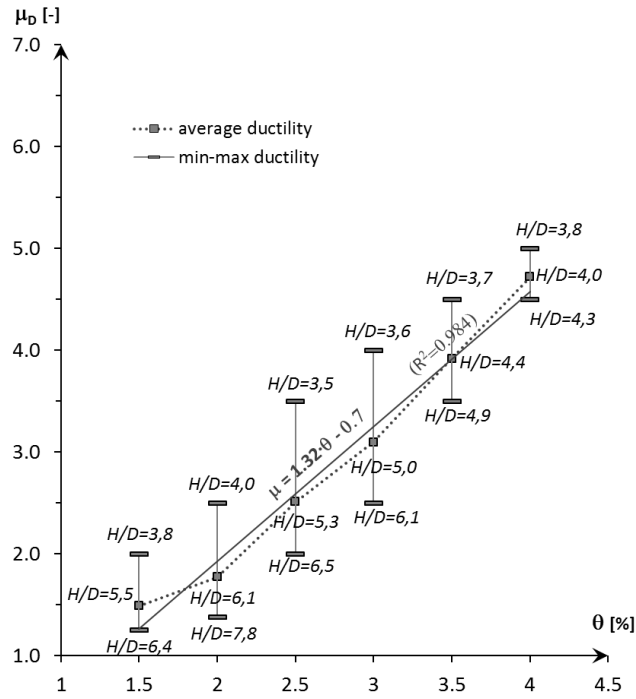
Fig. 16 Intervals for ductility demand, μ_Δ, versus drift, θ, obtained for the realistic, analyzed design cases, and interpolating line approximating values corresponding to medium T_{eff} values of the design intervals
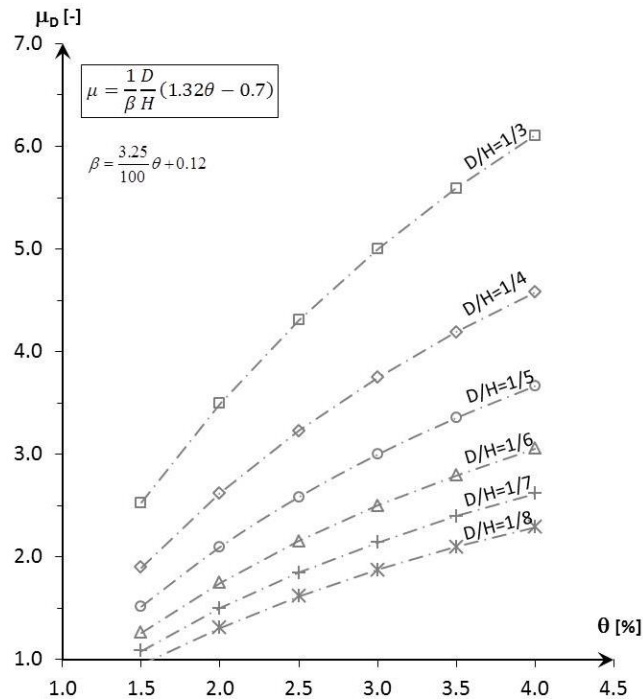

Fig. 17 Approximate relation for μ_Δ versus drift θ, and curves obtained for some pre-defined values of H/D (Eqs. (30)-(31))

With reference to the realistic, analyzed design cases, it was possible to plot the intervals in ductility, $\mu_{\Delta,min}$-$\mu_{\Delta,max}$, and the mean values of these, $\mu_{\Delta,mean}$, corresponding to prefixed drift values (see Fig. 16).

It is deduced that higher drifts, θ, are tied to high displacement ductility values, μ_Δ. With (H/D) ratio values between 4 and 5, drifts $\theta \geq 3$-3.5% correspond to ductility $\mu_\Delta \geq 3.5$, that is the upper limit currently adopted by seismic codes for bridge piers; thus, higher drift design requirements imply a strong inelastic behavior by the RC members.

Observing the ductility ratio between the medium value, $\mu_{\Delta,mean}$, and the extreme value of the interval, $\mu_{\Delta,min}$ or $\mu_{\Delta,max}$, corresponds approximately to the ratio between the corresponding mean values of (D/H), it was possible to derive the more general relation, given by Eqs. (30)-(31), and plot a series of curves for prefixed (D/H) values, extending the previously obtained ranges (see Fig. 17)

$$\mu = \frac{1}{\beta} \frac{D}{H} \left(1.32\vartheta - 0.7\right) \tag{30}$$

where

$$\beta = \frac{3.25}{100}\vartheta + 0.12 \tag{31}$$

with θ expressed in percentage (%).

To obtain Eqs. (30)-(31), the equations given by linear interpolation of $\mu_{\Delta,mean}$ values (Fig. 16) and of (D/H) mean values, plotted versus drift, were used. These mean values of (D/H) were calculated, for the various drift levels examined, performing new, realistic, design cases, in which the values of displacement ductility obtained by equation in Fig. 16 were used as input parameters.

The proposed equations are functional to a direct estimation of the method accuracy on the base of the design drift: once the design drift θ for the RC bridge bent is decided by the designer, the related design ductility μ_D can be derived using Eq. (30), and the diagram in Fig. 15 can be entered to derive the expected accuracy of the simplified procedure.

5. Conclusions

This work provides an estimate of the current DDBD method accuracy for simple SDOF structures, with specific reference to isostatic bridges, in which single-column RC bents generally conform to the assumptions valid for simple SDOF systems.

The method is shown to be generally conservative, at least for structures with $T_{eff} < 3.0$ s. Underestimation errors are never relevant, being at most limited to around 10% for any realistic design case. On the contrary, overestimation errors depend significantly on design ductility level: for low-medium ductility design cases ($\mu_D \leq 1.5$), the DDBD method is still very accurate, ($E_m < +10\%$), while for higher ductility values ($1.5 < \mu_D \leq 3.5$), more significant error levels tend to be attained, but they are still acceptable considering the implicit simplification of the equivalent linear DDBD procedure ($E_m < 20$-30% in nearly all the design cases). A medium error diagram as a function of design ductility, μ_Δ^d and effective period, T_{eff} is presented to summarize the scatter in the results.

Finally, as a useful tool for the DDBD design process, an approximate relationship between

ductility and drift is presented, since it is functional to a direct estimation of the accuracy in relation to the choice of the design drift level.

References

Ayala, G.A., Castellanos, H. and Lopez, S. (2012), "A displacement-based seismic design method with damage control for RC buildings", *Earthq. Struct.*, **3**(3), 413-434.

Chopra, A.K. (2001), "Direct displacement-based design: use of inelastic vs. elastic design spectra", *Earthq. Spectra*, **17**(1), 47-64.

Comité Européen de Normalisation, EN 1998-1 (2003), Eurocode 8, *Design of Structures for Earthquake Resistance" - Part 1: "General Rules, Seismic Actions and Rules for Buildings*, CEN, Brussels, Belgium.

Comité Européen de Normalisation, prEN 1998-1 (1998), Eurocode 8, *Design of Structures for Earthquake Resistance" - Part 1: "General Rules, Seismic Actions and Rules for Buildings*, CEN, Brussels, Belgium.

Dwairi, H.M., Kowalsky, M.J. and Nau, J.M. (2007), "Equivalent damping in support of direct displacement-based design", *J. Earthq. Eng.*, **11**(4), 512-530.

Faccioli, E. and Villani, M. (2009), "Seismic hazard mapping for Italy in terms of broadband Displacement Response Spectra", *Earthq. Spectra*, **25**(3), 515-539.

Fajfar, P. and Krawinkler, H. (1997), "Seismic design methodologies for the next generation of codes", *Workshop on Seismic Design Methodologies for the Next Generation of Codes*, Bled, Slovenia.

Grant, D.N., Blandon, C.A. and Priestley, M.J.N. (2005), *Modelling Inelastic Response in Direct Displacement-Based Design*, Report 2005/03, IUSS Press, Pavia, Italy.

Grendene, M., Franchetti, P. and Modena, C. (2012), "Regularity criteria for RC and PRC multispan continuous bridges", *J. Bridge Eng.*, **17**(4), 671-681.

Italian Ministry of Infrastructure, D.M. Infrastrutture 14 gennaio 2008, NTC '08, "Nuove Norme Tecniche per le Costruzioni", published on S.O. n. 30 in G.U. n. 29.

Jacobsen, L.S. (1930), "Steady forced vibrations as influenced by damping", *Transactione*, ASME, **52**(1), 169-181.

Jacobsen, L.S. (1960), "Damping in composite structures", *Proceedings of the 2nd World Conference on Earthquake Engineering*, Tokyo and Kyoto, Japan.

Newmark, N.M. and Hall, W.J. (1982), *Earthquake Spectra and Design*, Monograph, Earthquake Engineering Research Institute (EERI), Oakland, California, USA.

Priestley, M.J.N. (1993), "Myths and fallacies in earthquake engineering-conflicts between design and reality", *Bull. NZSEE*, **26**(3), 329-341.

Priestley, M.J.N. (2000), "Performance based seismic design", Keynote Address, *Proceedings of the 12th World Conference on Earthquake Engineering*, Auckland, New Zealand.

Priestley, M.J.N. (2005), "Viscous damping in seismic design and analysis", *J. Earthq. Eng.*, **9**(2), 229-255.

Priestley, M.J.N., Calvi, G.M. and Kowalsky, M.J. (2007), *Displacement-Based Seismic Design of Structures*, IUSS Press, Pavia, Italy.

Shibata, A. and Sozen, M. (1976), "Substitute-structure method for seismic design in reinforced concrete", *J. Struct. Div.*, ASCE, **102**(1), 1-18.

Sullivan, T.J., Priestley, M.J.N. and Calvi, G.M. (2012), *A Model Code for the Displacement-Based Seismic Design of Structures, DBD 12*, IUSS Press, Pavia, Italy.

CC

Abbreviations

A_c	area of concrete section
$a_u{}^d$	ultimate design acceleration
a_y	yield acceleration
C	generic constant
D	diameter of pier circular section
D.K.	Equivalent Viscous Damping model by Dwairi *et al.* (Dwairi *et al.* 2007)
D.K.G.	Equivalent Viscous Damping model by Dwairi *et al.* with correction factor for elastic damping (Priestley *et al.* 2007)
d_{bl}	longitudinal reinforcement diameter
E	relative error (%), by Eq. (16), between design displacement ($\Delta_u{}^d$) and average inelastic displacement obtained by TH analyses ($\Delta_u{}^{TH}$)
E_m	medium relative error (%), by polynomial interpolation of relative error curves in plane E-T_{eff}
ESDOF	Equivalent Single Degree Of Freedom
EVD	Equivalent Viscous Damping model
f'_c	compressive strength of unconfined concrete
f'_{ce}	expected concrete compressive strength
$F_u{}^d$	ultimate force/strength relative to design displacement, $\Delta_u{}^d$
f_y	characteristic yield stress of steel
f_{ye}	expected yield stress of steel
G.B.P.	Equivalent Viscous Damping model by Grant *et al.* (Grant *et al.* 2005)
H	height of pier
(H/D)	height/diameter ratio of pier
JDSS	Equivalent Viscous Damping model by Jacobsen (Jacobsen 1930, 1960)
K	structure stiffness
K_{eff}	structure effective stiffness for DDBD
L_{sp}	strain penetration length
M_{01}	flexural moment at pier top
M_{02}	flexural moment at pier bottom
M_{1eff}	ESDOF effective mass for case study 1
M_{2eff}	ESDOF effective mass for case study 2
M_{base}	sum of moments at base level
M_{eff}	effective mass of ESDOF
N_{Ed}	design axial load
P	axial force on section (also N)
q	behavior factor
r_m	factor of first order distribution of flexural moments at pier top and bottom
r_Δ	post-yielding displacement bilinear factor
R_ξ	reduction factor applied to displacement spectrum for damping ξ
S	soil factor
$S_a(T)$	elastic Acceleration Response Spectrum
$S_{a\xi}(T)$	design or over-damped Acceleration Response Spectrum
SDOF	Single Degree Of Freedom
$S_\Delta(T)$	elastic Displacement Response Spectrum
$S_{\Delta 0.05}(T)$	5% damped Displacement Response Spectrum
$S_{\Delta\xi}(T)$	design or over-damped Displacement Response Spectrum
T_B	period at beginning of maximum spectral response acceleration plateau
T_C	period at end of maximum spectral response acceleration plateau
T_D	period parameter ("corner period" of displacement response spectrum)

T_{eff}	effective period of SDOF system at its design displacement
$T_{eff,max}$	upper limit of admissible T_{eff} values, for fixed values of θ and μ_Δ^d, for realistic design cases
$T_{eff,min}$	lower limit of admissible T_{eff} values, for fixed values of θ and μ_Δ^d, for realistic design cases
T_{el}	elastic period of SDOF substitute system
TT	Takeda Thin hysteretic model
α	unloading stiffness factor in modified Takeda model
β	reloading stiffness factor in modified Takeda model
Δ_u	ultimate displacement
Δ_u^d	ultimate target displacement
Δ_u^{TH}	ultimate displacement obtained by using NLTH analysis
Δ_y	yield displacement
ε_c	concrete compressive strain limit
ε_s	ultimate strain of longitudinal reinforcement
ε_y	yield reinforcement stress
θ	drift ratio
θ_d	design drift ratio
λ	coefficient of slenderness
λ_{lim}	limit value of slenderness coefficient (D.M. Infrastrutture 14 gennaio 2008 - NTC '08)
μ_Δ	displacement ductility factor
μ_Δ^d	design displacement ductility factor
$\mu_{\Delta,max}$	maximum value of displacement ductility related to a fixed value of drift
$\mu_{\Delta,mean}$	mean value of displacement ductility related to a fixed value of drift
$\mu_{\Delta,min}$	min value of displacement ductility related to a fixed value of drift
v	normalized axial load
ξ	fraction of critical damping
ξ_{el}	elastic viscous damping
ξ_{eq}	equivalent viscous damping
ξ_{hyst}	hysteretic component of equivalent viscous damping ratio
ρ_l	area ratio of longitudinal reinforcement
Φ_y	nominal yield curvat